Pol. J. Environ. Stud. Vol. XX, No. X (XXXX), 1-12
DOI: *10.15244/pjoes/205257* ONLINE PUBLICATION DATE: 2025-07-12

Original Research

Experimental Removal of *Microcystis aeruginosa* by Magnetic Clay Minerals Synergized with CPAM and Adsorption Mechanism Study

Tingyu Fan[1, 2]*, Xuyang Zhou[1, 2], Pingjuan Wu[1, 2], Akang Lu[1, 2]

[1]School of Earth and Environment, Anhui University of Science and Technology, Huainan, 232001, China
[2]Anhui Engineering Laboratory for Comprehensive Utilization of Water and Soil Resources and Ecological Protection in Mining Area with High Groundwater Level, Huainan, 232001, China

Received: 10 February 2025
Accepted: 17 May 2025

Abstract

Cyanobacterial blooms, a harmful consequence of water eutrophication, necessitate efficient algal removal strategies. This study synthesized magnetic bentonite and kaolinite via co-precipitation by loading nano-Fe_3O_4 onto clay minerals. The materials were characterized using SEM, FTIR, and XRD: single-factor experiments and response surface methodology (Box-Behnken design) optimized parameters for algae removal. Optimal conditions included a 1:1 ratio of magnetic clay minerals to cationic polyacrylamide (CPAM), pH 2, 10 min stirring (150 rpm), and dosages of 0.8 g/L (magnetic bentonite) and 0.4 g/L (magnetic kaolinite). Further refinement via response surface analysis yielded 92.13% algal cell removal with magnetic bentonite at 0.206 g/L, 12.9 min stirring, and 170.6 rpm. Mechanistic studies (Zeta potential, SEM, particle size analysis) indicated that electrostatic adsorption between algae and magnetic clays formed flocs, subsequently captured by CPAM networks. This rapid, efficient process highlights the potential of magnetic clay-CPAM composites for treating eutrophic, algae-laden waters. The findings offer a technical reference for sustainable water remediation.

Keywords: eutrophication, flocculation and algae removal, magnetic clay minerals, CPAM, adsorption mechanism

Introduction

Eutrophication is one of the most common water environmental issues [1]. Algal blooms reduce the concentration of dissolved oxygen and water transparency, affecting the growth and reproduction of aquatic organisms [2]. Cyanobacterial blooms are a common type of eutrophic algae. Due to the morphology and electronegativity of algal cells, as well as extracellular organic secretions, traditional treatment methods struggle to remove algal cells because of electrostatic repulsion, making it difficult for flocs to form [3].

In recent years, due to the natural clay materials with montmorillonite cells formed in the layered structure of the presence of certain cations (Cu, Mg, Na, K, etc.),

*e-mail: ayufty@163.com
Tel: 0554-6631021

and the role of these cations and montmorillonite cells is very unstable, with good ion exchange [4]. Its greater adsorption properties and lower acquisition costs have been widely used in water treatment [5]. However, in terms of algal removal, the adsorption properties of clay minerals are not enough to cope [6]. For this reason, Limei et al. [7] and Ping et al. [8] used inorganic and organic modification methods of clay mineral surface loading with polymerized ferric-lanthanum sulfate and cationic surfactant (DPQAC), respectively, to increase the active sites on the surface of clay minerals in order to enhance the adsorption capacity of clay minerals for algae. It was found that the composite-modified bentonite (PFS-La) modified with polymerized ferric-lanthanum sulfate achieved a chlorophyll a removal rate of 80.4% at 0.3g/L. Organic kaolin and organic bentonite modified with a novel cationic surfactant (DPQAC) at a dosage of 0.03 g/L could remove 100% of red tide *Heterobasidium* in 24 h. Shanshan [9] used a biological modification method involving *Bacillus amyloliquefaciens* to lyse algal cells, enhancing the adsorption capacity of clay minerals towards algae. The study found that when the pH was 8.0, the dosage was 1.16 g/L, and the initial concentration of *Microcystis aeruginosa* was 5.0 mg/L, the algal removal efficiency reached 96.09%. However, water treatment in the slow settlement of clay is difficult to recycle and easily causes secondary pollution; solving this problem has become the key to applying clay minerals in the treatment of eutrophication in water bodies [10].

Most natural clay minerals have negatively charged surfaces [11], and algal cells are also negatively charged [12]. Electrostatic repulsion leads to low efficiency and high usage of clay minerals when removing algal cells [13]. Cationic polyacrylamide (abbreviated "CPAM"), an organic cationic polymer flocculant, can effectively combine with negatively charged suspended algae in water to improve flocculation [14]. However, when used alone, its flocs have poor sedimentation performance. Magnetic nano-Fe_3O_4 particles are superparamagnetic at room temperature and can be quickly separated from the liquid phase by an external magnetic field [15]. However, their small particle size, tendency to agglomerate, and lack of surface functional groups limit their effectiveness as standalone flocculants [16].

This study selected bentonite and kaolinite, two natural clay minerals, and prepared magnetic clay minerals using the co-precipitation method. The surface characteristics of the materials were analyzed, and the removal efficiency and mechanism of *Microcystis aeruginosa* in the presence of cationic polyacrylamide (CPAM) were investigated. This provides technical support for using magnetic clay minerals to manage water eutrophication.

Materials and Methods

Materials

Materials: Bentonite and kaolinite (200 mesh) were purchased from Henan Hengyuan New Materials Co., Ltd. Ferric chloride hexahydrate ($FeCl_3 \cdot 6H_2O$), ferrous chloride tetrahydrate ($FeCl_2 \cdot 4H_2O$), ammonia, anhydrous ethanol, and cationic polyacrylamide (CPAM) were all analytical-grade reagents. The water used in the experiments was purified.

Instruments: FE28-Standard pH meter, H1850 high-speed centrifuge, 721G visible spectrophotometer, LC-ES-60 electric stirrer, THZ-82A thermostatic water bath shaker, and 101-1B oven.

Synthesis of Magnetic Clay Minerals

Magnetic clay minerals were synthesized using the co-precipitation method. One gram of bentonite was added to 100 ml of distilled water and sonicated for 10 minutes to achieve complete dispersion. Then, 1.96 g of $FeCl_3 \cdot 6H_2O$ and 0.9 g of $FeCl_2 \cdot 4H_2O$ were added, followed by stirring for 10 minutes until completely dissolved. The pH was then adjusted to 10-11 using $NH_3 \cdot H_2O$, and the mixture was stirred at 60ºC for 3 hours. Afterward, a permanent magnet was used for separation, followed by washing three times with ethanol and distilled water. The product was dried at 65ºC, ground, and labeled magnetic bentonite (p/f). Magnetic kaolinite was prepared using the same procedure and labeled as (g/f).

Characterization Methods for Magnetic Clay Minerals

A Hitachi FlexSEM1000 scanning electron microscope (SEM) was used to observe the morphology of the samples before and after modification and flocculation adsorption. The composition of the samples was analyzed with a Thermo Nicolet Model Nexus 670 infrared spectrometer. The crystal structure and composition of the powdered samples were characterized using a Bruker D8 Advance X-ray diffractometer. The particle size and Zeta potential of magnetic clay minerals and *Microcystis aeruginosa* before and after flocculation were measured using a Benano 90 Zeta nanoparticle size and Zeta potential analyzer from Dandong Baite.

Cultivation of Microcystis Aeruginosa

Microcystis aeruginosa used in this study was obtained from the Freshwater Algae Culture Collection of the Chinese Academy of Sciences, catalog number FACHB-315. The algae were transferred to a 100 ml sterile glass Erlenmeyer flask for scaling up the culture using BG11 medium. Algal cell density was measured using a hemocytometer, and a calibration curve

was established by plotting the absorbance of algal cells at λ = 680 nm against the cell count to establish a functional relationship.

Single-Factor Experiments for Optimal Removal Efficiency

50 ml of diluted *Microcystis aeruginosa* solution was placed in a 100 ml. Different single factors were used as experimental variables to study the optimal algal removal effect of magnetic clay minerals (the experimental design is shown in Table 1). The pH of the 50 mL algal suspension was adjusted by dropwise addition of 0.1 mol/L HCl or NaOH under continuous stirring at 150 rpm until the target pH (2.0-10.0) was achieved. For the extreme acidic condition (pH = 2.0), a 0.01 mol/L KCl-HCl buffer (pH 2.0, buffer capacity β = 0.05 mol/L) was supplemented to ensure pH stability. No buffering agents were employed under other pH conditions to avoid introducing additional ions that might interfere with the adsorption process. After adsorption and sedimentation, the supernatant was collected, and its absorbance at 680 nm was measured using a UV spectrophotometer to calculate the removal rate. All experiments were conducted at room temperature.

The algal cell removal rate is calculated using the following formula:

$$R = \frac{x_0 - x_1}{x_0} \times 100 \quad (1)$$

In the formula, R is the algal cell removal rate, expressed as a percentage; x_0 is the initial algal cell concentration, 10^6 cells/mL; and x_1 is the algal cell concentration after treatment, 10^6 cells/mL.

Zeta Potential Measurement

25 ml of distilled water was mixed with 0.01 g of each of the two types of modified magnetic materials before and after modification. The pH was adjusted to a range of 2-10 using 0.1 mol/L HCl and NaOH. After ultrasonic dispersion for 3 minutes, the Zeta potential values of the two materials and *Microcystis aeruginosa* at different pH levels were measured using a Benano 90 Zeta potential analyzer.

Results and Discussion

Characterization of Magnetic Clay Minerals

SEM Analysis

Scanning electron microscope (SEM) images of the clay minerals and magnetic clay minerals are shown in Fig. 1(a-d). After modification, the clay minerals exhibit irregular block shapes with fine micropores on their surfaces, which increases their specific surface area and enhances adsorption capacity. Both magnetic clay minerals have surfaces uniformly covered with numerous fine particles at the nanoscale, indicating that the nanoscale Fe_3O_4 microspheres prepared by co-precipitation have a good size uniformity and are well loaded onto the clay mineral surfaces. The particle size is approximately 20 nm, and the synthesized magnetic clay minerals exhibit a porous structure that improves the material's adsorption performance [17].

FTIR Analysis

The FTIR spectra of the two natural clay minerals are shown in Fig. 1e). The broad adsorption band at around 3400 cm^{-1} in bentonite is caused by the vibration of O-H bonds and hydroxyl groups in the ligand water structure [18]; the absorption peaks near 1630 cm^{-1} likewise belong to the deformation vibration of adsorbed H_2O, and the peaks at 1034 cm^{-1} likewise originate from fluctuations of Si-O-Si rings in SiO_4 tetrahedra. Similarly, the absorption peaks at 3694 cm^{-1} and 3620 cm^{-1} in kaolinite are caused by the stretching vibration of the Al-O-Al group [19], and the absorption peak at 1628 cm^{-1} comes from the bending vibration of the O-H coordination water molecule [20]; the peaks observed at 1029 cm^{-1} and 544 cm^{-1} are caused by the stretching vibration of Si-O-Si and Si-O-Al stretching vibrations; the characteristic peaks at 795 cm^{-1}, 753 cm^{-1}, and 544 cm^{-1} are A superposition of the characteristic vibrations of magnesium and aluminum oxides [21], and the absorption peak at 915 cm^{-1} is attributed to the presence of hydroxyl groups in the material.

The FTIR profiles of the modified magnetic clay minerals are shown in Fig. 1f). Absorption peaks at 580 cm^{-1}, 541 cm^{-1}, 538 cm^{-1}, and 536 cm^{-1} were observed in both magnetic clay minerals, respectively,

Table 1. Table of one-way experimental design for optimal removal of magnetic clay minerals combined with CPAM.

One-factor	Level					
CPAM Dosage ratio	1:1	1:2	2:1	3:1	4:1	-
Dosage (g)	0.005	0.01	0.02	0.03	0.04	0.05
Stirring rate (r/min)	50	100	150	250	-	-
Mixing time (min)	1	3	5	10	15	-
pH	2	4	6	8	10	-

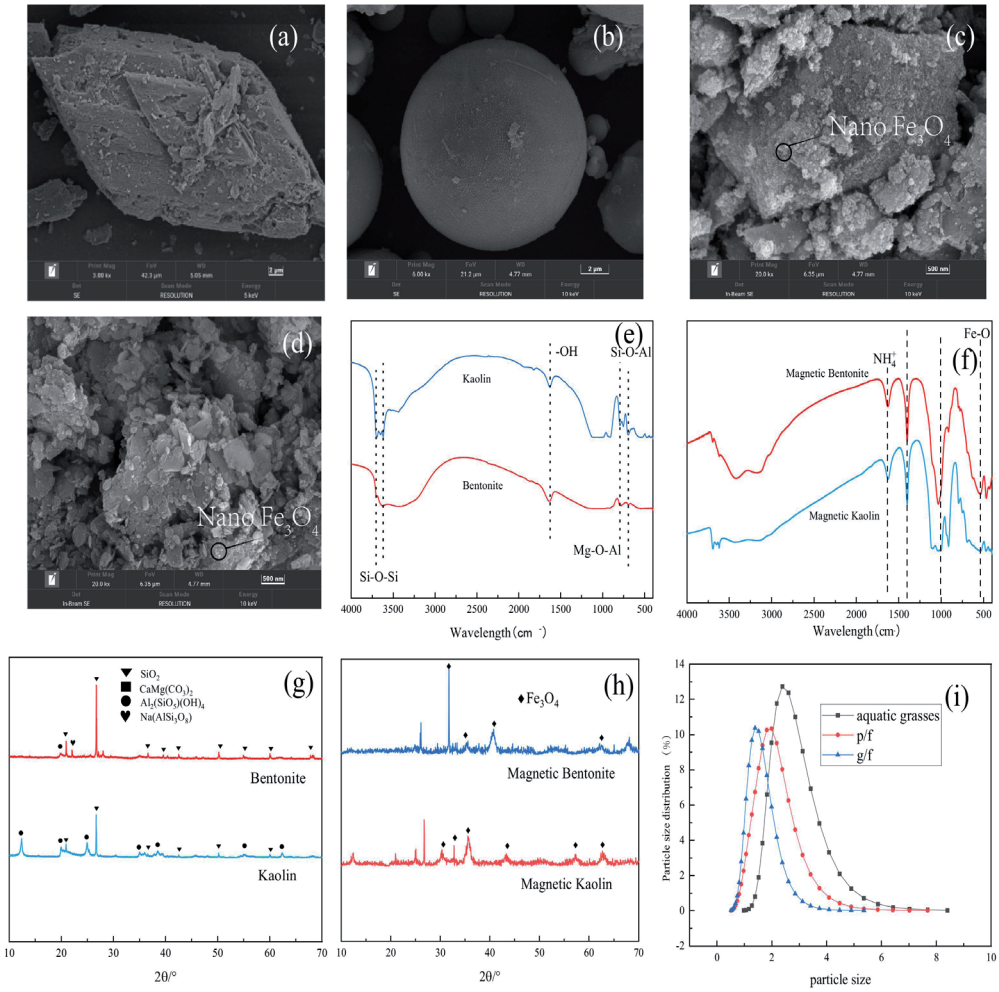

Fig. 1. Characterization of clay minerals before and after modification.
a) SEM image of bentonite. b) SEM image of kaolin. c) SEM image of magnetized bentonite. d) SEM image of magnetized kaolin. e) FTIR images of clay minerals. f) FTIR images of magnetic clay mineral. g) XRD images of clay minerals. h) XRD images of magnetic clay mineral. i) Particle size distribution of two magnetic clay minerals and algal cells of Microcystis aeruginosa.

which can be attributed to the stretching mode of Fe-O in Fe_3O_4 [22], proving that Fe_3O_4 has been successfully loaded onto the natural clay minerals. Compared with the infrared spectrograms of the natural clay minerals, the characteristic peaks of the natural clay minerals were retained in the magnetic clay minerals, which proved that the modification did not destroy the original structure of the materials. At the same time, a new narrow absorption band at 1400 cm^{-1} appears in both magnetic clay minerals, which may be caused by the asymmetric deformation vibration of NH_4^+, which is attributed to the involvement of ammonia in the synthesis of the materials, resulting in the presence of NH_4^+ on the surface of the materials.

XRD Analysis

The XRD pattern of the natural clay minerals is shown in Fig. 1g). Characteristic diffraction peaks of quartz appear at 2θ = 20.92°, 26.68°, 36.61°, 39.62°, 42.51°, 50.21°, 55.08°, and 60.02°, indicating that the primary component of the natural clay minerals is quartz [23]. In addition to quartz, the characteristic peaks of aluminosilicates (2θ = 19.77°) were also detected in bentonite and kaolinite.

The XRD pattern of the magnetic clay minerals is shown in Fig. 1h). Characteristic diffraction peaks appear near 2θ = 30.2°, 32.0°, 35.6°, 43.2°, 53.7°, 57.1°, and 62.7° for both magnetic clay minerals, corresponding to (220), (311), (400), (422), (511), and (440) lattice planes, respectively. These lattice planes are the standard pattern for crystalline magnetite with a spinel structure [24]; this demonstrates the successful loading of Fe_3O_4 onto natural clay minerals and the coarser characteristic peaks due to the generation of a large number of nanoparticles with a high specific surface area [25]. The diffraction peaks of the magnetic clay minerals did not undergo any particular changes compared to the natural clay mineral profiles, again indicating that the Fe_3O_4 modification of the clay minerals did not affect the material's structure.

Magnetic Clay Mineral Particle Size Analysis

The particle size distribution of the two magnetic clay minerals and the logarithmic growth phase of *Microcystis aeruginosa* cells is shown in Fig. 1i). The results indicate that the D50 values for magnetic bentonite, magnetic kaolinite, and *Microcystis aeruginosa* cells are 1.756 μm, 1.453 μm, and 2.403 μm, respectively. Research suggests that the particle size of materials affects the efficiency of algal cell recovery [26]. Smaller particle sizes result in a larger specific surface area and better adsorption capacity. Additionally, the settling speed of flocs after coagulation may depend on the particle size of the magnetic materials adsorbed onto the algal cells. Larger particle sizes generally lead to higher settling speeds, thereby improving algal cell recovery efficiency [27]. Studies using models have shown that magnetic materials with radii between 1-3 μm exhibit higher settling speeds [28]. The particle size analysis indicates that the magnetic clay minerals have a high specific surface area, and their particle sizes ensure a high settling speed of the flocs after coagulation, which facilitates the separation of algal cells.

Removal of Microcystis Aeruginosa by Magnetic Clay Minerals in Synergy with CPAM

Effects of Different Magnetic Material Dosage and CPAM Dosing Ratio

The variation in the removal rates of *Microcystis aeruginosa* with different dosages of the two magnetic clay minerals is shown in Fig. 2a). At a dosage of 0.1 g/L, the removal rates for magnetic bentonite and magnetic kaolinite were 88.36% and 88.09%, respectively. As the dosage increases, the removal rate also increases. The removal rate reaches a maximum of 95.76% for magnetic bentonite at a dosage of 0.8 g/L and 90.54% for magnetic kaolinite at 0.4 g/L. However, with further increases in dosage, the removal rate exhibits a slight decrease. This decline is attributed to the excessive amount of material, which can inhibit the adsorption of algae cells onto the magnetic materials, leading to reduced removal efficiency [29].

The changes in the removal rate of P. aeruginosa under different CPAM dosing ratios are shown in Fig. 2b). Magnetic bentonite and magnetic kaolin were less affected by the dosing ratio. The algal removal rate basically remained above 80% in the range of 1:2 to 4:1. When the dosing ratio of CPAM and magnetic clay minerals was 1:2, the amount of CPAM was not enough to make all the tiny flocs in the water coalesce into larger flocs, thus limiting the removal rate of *Microcystis aeruginosa*. With the increase of the dosing ratio, the removal rate of *Microcystis aeruginosa* is also increasing until the CPAM concentration is too high. At this time, too much CPAM, on the one hand, will lead to positively charged colloids in the water, and the repulsive force increases, thus making the colloid destabilizatio [30]; on the other hand, too much CPAM will greatly increase the viscosity of the solution so that solution mixing is insufficient but also impedes the flocculant's role in the net trapping [31]. So, a dosing ratio that is too large will also reduce the removal rate of *Microcystis aeruginosa*. Combining the economic cost and the actual removal effect, the optimal dosing ratio is 1:1, in which the removal rate of two magnetic clay minerals on *Microcystis aeruginosa* is 86.89% and 83.62%, respectively.

Effect of Different Mixing Times and Mixing Rates

The variation in algal cell removal rates of the two magnetic clay minerals at different stirring times is shown in Fig. 2c). As the stirring time increases, the removal rate first increases and then decreases, reaching a maximum value in 10 minutes. At this time, the removal rates for the two magnetic clay minerals are 88.66% and 95.13%, respectively. When the stirring time is too short, there is insufficient contact between *Microcystis aeruginosa* and the magnetic clay minerals, resulting in a lower removal rate. Conversely, if the stirring time is too long, although the algae and magnetic clay minerals are well mixed, the flocs will likely break apart again, reducing the removal rate [32]. Additionally, longer stirring times lead to increased time and economic costs, making 10 minutes the optimal stirring duration.

The variation in the removal rates of algal cells by the two magnetic clay minerals at different stirring speeds is shown in Fig. 2d). The removal rate initially increases with stirring speed and then decreases, reaching a maximum of 150 rpm, with removal rates of 94.23% and 90.53%, respectively. At lower stirring speeds, the removal rate is significantly lower; for example, at 50 rpm, the removal rate for magnetic kaolinite is only 51.23%. This is because a low stirring speed results in uneven distribution of the magnetic clay minerals and algal cells, leading to inadequate mixing. Conversely, at excessively high stirring speeds, the impact forces generated can disperse and disintegrate the flocs, reducing the removal efficiency of *Microcystis aeruginosa*. Moreover, very high stirring speeds may cause the rupture of algal cells, releasing toxins and potentially causing secondary damage to the aquatic environment [33]. Therefore, a stirring speed of 150 rpm is considered optimal.

Removal Rates at Different pHs

The removal efficiency of *Microcystis aeruginosa* by the two magnetic clay minerals at different pH levels and the Zeta potential values before and after modification are shown in Fig. 2e). As pH increases, the removal rate first decreases and then increases, with the minimum rate occurring in the neutral pH range. The lowest removal rates for the two magnetic clay minerals were 78.48% and 62.80%, respectively. At pH = 2, magnetic

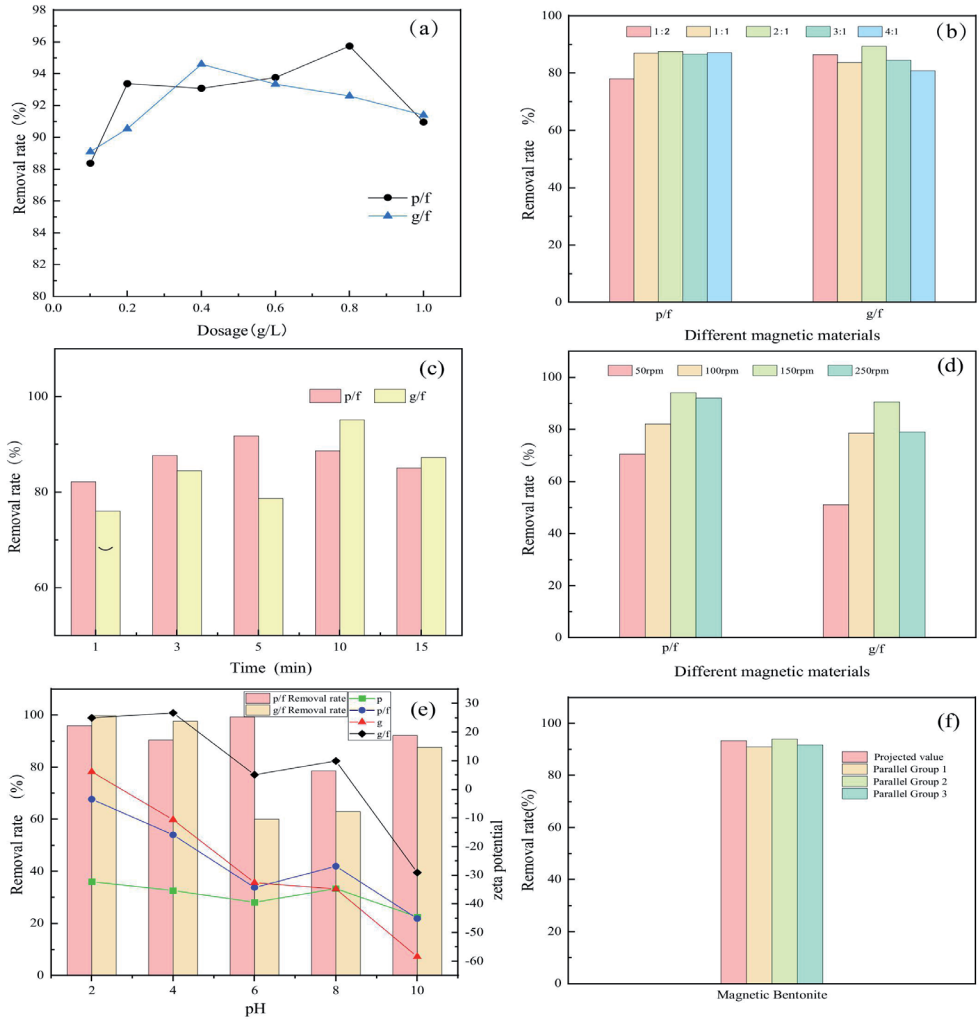

Fig. 2. Plot of results of one-way experiments.
a) Changes in the removal rate of Microcystis aeruginosa at different dosages. b) Effects of different CPAM dosing ratios on the removal rate of Microcystis aeruginosa. c) Effect of different stirring times on the removal of Microcystis aeruginosa. d) Effect of different agitation rates on the removal of algal cells. e) Changes in Microcystis aeruginosa removal rate at different pH and changes in zeta potential before and after modification. f) Response surface optimization of predicted and actual values for optimal removal conditions of magnetic bentonite clay.

bentonite and magnetic kaolinite exhibit excellent removal efficiencies of 95.83% and 99.59%, respectively. Notably, as the pH increases from 8 to 10, the removal rate of *Microcystis aeruginosa* shows an increasing trend. This may be due to the Zeta potentials of the two magnetic clay minerals at pH = 10, which are -45.19 mV and -29.14 mV, respectively. The magnetic clay minerals at this pH carry strong negative charges that repel the similarly negatively charged *Microcystis aeruginosa* cells, partially hindering flocculation. However, cationic polyacrylamide (CPAM), an organic cationic flocculant, contains numerous cationic functional groups. These cationic groups have a strong electrostatic attraction to the negatively charged magnetic clay minerals and algal cells, overcoming the electrostatic repulsion and thereby enhancing the removal rate of *Microcystis aeruginos* [34].

Response Surface Optimization Experiment

The magnetic bentonite, which showed better algae cell removal performance among the two magnetic clay minerals, was selected for response surface optimization experiments. The aim was to optimize the conditions for algae cell removal using the magnetic clay mineral flocculation system and to determine the optimal process parameters. Stirring time (minutes), rotation speed (rpm), and the added amount of magnetic natural clay minerals (g/L) were selected as controllable variables A, B, and C, respectively, while the algae cell removal rate (%) was the response value. A total of 17 experiments were designed using the Box-Behnken method and analyzed using a quadratic regression model.

The accuracy of the quadratic model for magnetic bentonite was found to be high. As shown in Table 2, the model has an R^2 value of 0.97098, indicating that

Table 2. Response Surface Optimization for Optimal Removal of Magnetic Bentonite Quadratic Model Error Statistical Analysis Table.

Parameters	Value	Parameters_1	Value_2
Std. Dev.	1.541104	R-Squared	0.970985
Mean	86.17647	Adj R-Squared	0.933679
C.V. %	1.788311	Pred R-Squared	0.623944
PRESS	215.4688	Adeq Precision	16.18058

the model cannot explain less than 3% of the overall experimental variability. The adjusted R^2 and predicted R^2 values were 0.9337 and 0.6239, respectively, demonstrating that the model adequately describes the experimental process. Additionally, the model's CV value is approximately 1.78%, with a signal-to-noise ratio of 16.18058, indicating that the information explained by the model is about 16 times greater than that which cannot be explained, further proving the model's reliability. Moreover, as shown in Table 3, the model's PPP value is 0.000143 ($p<0.01$), indicating high significance. The impact of the three factors on the removal of *Microcystis aeruginosa* cells is ranked as follows: B>C>A, where rotation speed>dosage>stirring time. The linear equation represents the final simulated model result:

$$R = 74.89063 - 1.13750A + 0.23687B - 35.31250C + 0.00625AB + 0.625AC + 0.01875BC - 0.11750A^2 - 0.000918B^2 + 20.3125C^2 \quad (2)$$

The regression equation obtained from the model fitting identifies the optimal parameters for removing *Microcystis aeruginosa* using magnetic bentonite: stirring time of 12.9 minutes, rotation speed of 170.6 rpm, and dosage of 0.206 g/L. Under these conditions, the model predicts a removal rate of 93.29% for algae cells.

The optimal process parameters were revised to a stirring time of 13 minutes, a rotational speed of 170 rpm, and a dosage of 0.20 g/L for ease of operation. Three experiments were carried out under these conditions, as shown in Fig. 2f). The average algal cell removal rate of 92.13% was obtained, with a relative error of 1.16% from the model, which was small and verified the reliability of the model.

Algae Removal Mechanism Analysis

Zeta Potential

The Zeta potentials of the two magnetic clay minerals and *Microcystis aeruginosa* at different pH levels are shown in Fig. 3a). The Zeta potential values show that the Zeta potential of clay minerals generally decreases with increasing pH before and after modification. The Zeta potential of the unmodified clay minerals is negative across the entire pH range. After modification, the Zeta potential increases due to the positive charge from the nano-Fe_3O_4 loaded onto the clay minerals (attributed to the residual amino groups on the surface of nano-Fe_3O_4 during synthesis [35]), enabling the magnetic clay minerals to exhibit a positive surface charge under acidic conditions. As shown in Fig. 3, *Microcystis aeruginosa* secretes

Table 3. Response surface optimization magnetic bentonite model ANOVA table.

Source of variance	Squared sum	Degrees of freedom	Mean-square sum	F Value	P Value
Regression models	556.34	9	61.81	26.02	0.00014
A-Mixing time	0.125	1	0.125	0.052	0.8251
B-Number of revolutions per minute	78.12	1	78.125	32.89	0.0007
C-Dosage	32	1	32	13.47	0.0079
AB	39.06	1	39.06	16.45	0.0048
AC	1.56	1	1.56	0.65	0.4440
BC	0.56	1	0.56	0.24	0.6413
A^2	36.33	1	36.33	15.29	0.0058
B^2	355.41	1	355.41	149.65	< 0.0001
C^2	2.78	1	2.77	1.17	0.3151
Residual	16.62	7	2.37	-	-
Lost proposal	13.12	3	4.37	5	0.0770
Pure error	3.5	4	0.87	-	-
Total error	572.97	16	-	-	-

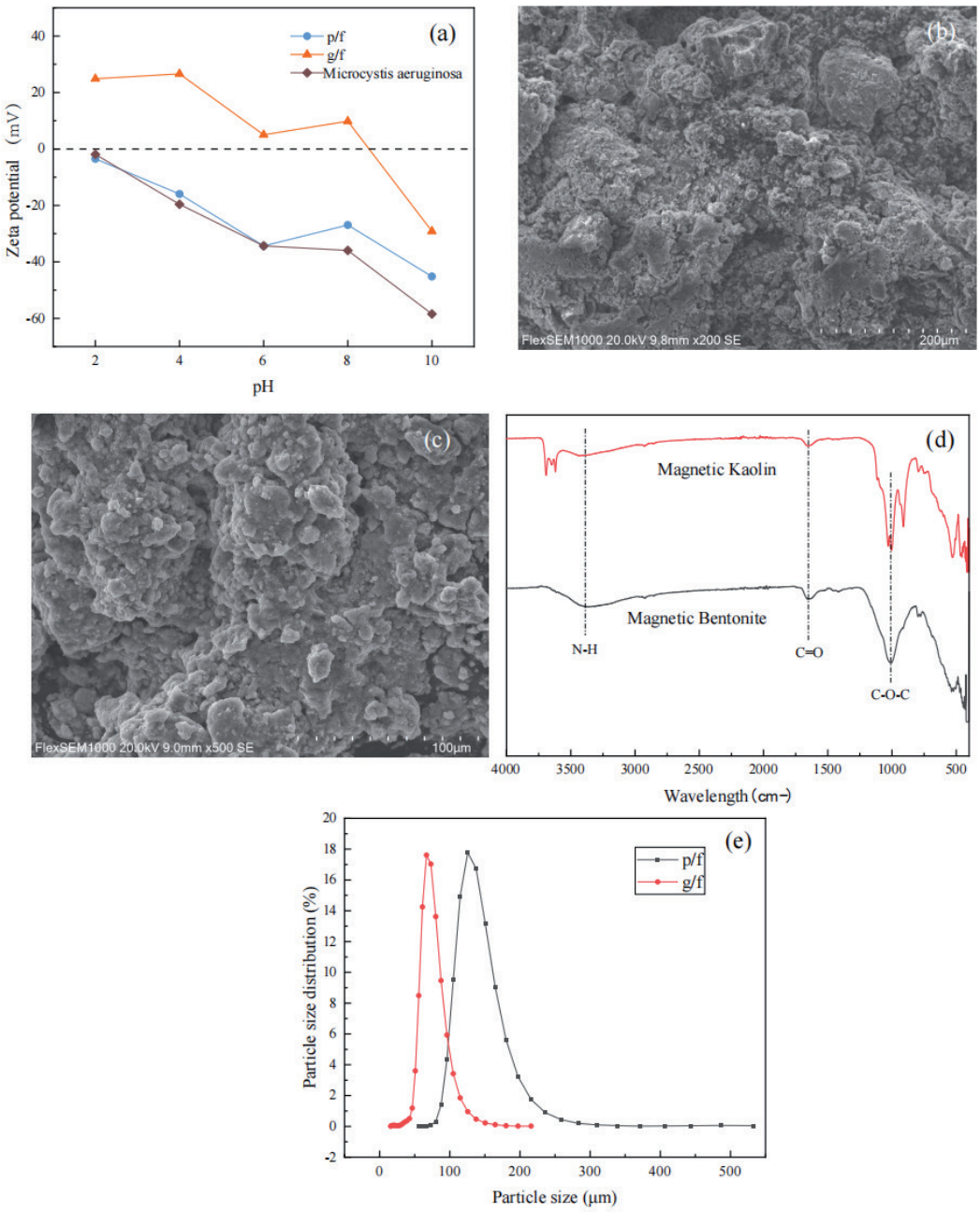

Fig. 3. SEM images of magnetic clay minerals combined with CPAM flocculation for algae removal. a) Zeta potentials of magnetic clay minerals and Microcystis aeruginosa at different pHs. b)Magnetic Bentonite; c) Magnetic Kaolin. d) FTIR images after adsorption. e) Particle size distribution of magnetic clay minerals after adsorption of Microcystis aeruginosa algal cells.

a large amount of negatively charged organic matter (AOMs) during its growth, which attaches to the cell surface, resulting in a high negative charge across all pH levels [36]. At pH = 10, *Microcystis aeruginosa* exhibits the lowest Zeta potential of -58.44 mV. Therefore, under acidic conditions, the positive surface charge of the magnetic clay minerals and the negative surface charge of *Microcystis aeruginosa* cells attract each other, creating a strong electrostatic force that helps the cells and magnetic materials to coagulate into larger flocs, thereby improving the removal efficiency of *Microcystis aeruginosa* [37].

Flocculation Mechanism for Algae Removal and Analysis of Influencing Factors

A high molecular weight polymer, CPAM carries numerous positive charges on its surface, exhibiting cationic polyelectrolyte properties [38]. It can form flocs through electrostatic adsorption with negatively charged algae cells. Clay minerals, when loaded with nano Fe_3O_4, shift from negative to positive surface charge, creating a positively charged system centered around the clay mineral particle [39]. Modified magnetic clay combined with CPAM can electrostatically adsorb

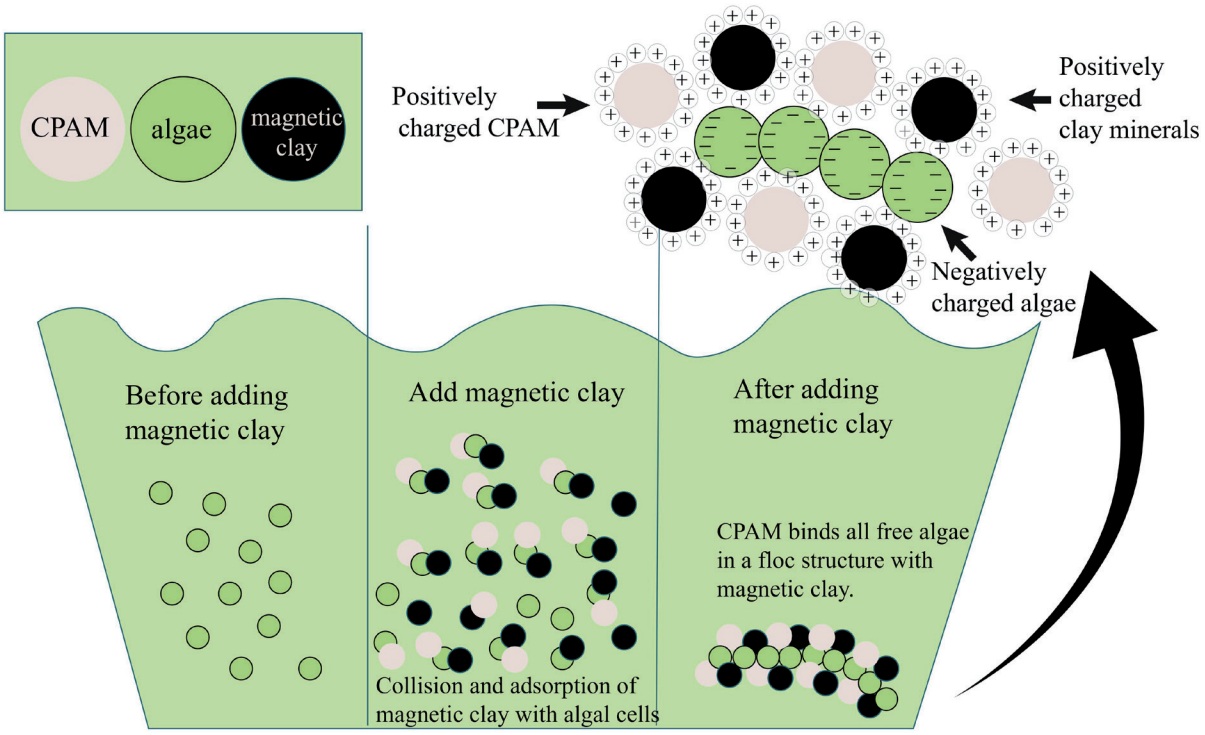

Fig. 4. Mechanism diagram of CPAM combined with magnetic clay minerals flocculation and algae removal process.

algae cells to form flocs. The process of algae removal through flocculation using magnetic clay combined with CPAM is illustrated in Fig. 4.

Additionally, as a long-chain polymer, CPAM facilitates floc formation through "adsorption-bridging" and "adsorption charge neutralization" between modified clay minerals and algae cells under van der Waals forces [40]. However, the effect of polymer dosage on flocculation is not linear. When the dosage is too low, it cannot effectively bridge and adsorb two colloidal particles. Conversely, an excess of polymer can lead to "colloid protection", preventing colloidal particles from aggregating and resulting in highly dispersed flocs [41]. Moreover, when CPAM is used alone as a flocculant for algae removal, the flocs formed are loose and light, making rapid sedimentation difficult [14]. Introducing magnetic clay minerals not only increases the compactness of the flocs but also significantly reduces the sedimentation time. Algae cells that settle to the bottom are deprived of light and cannot photosynthesize, while the hypoxic conditions at the water bottom further induce cell apoptosis or necrosis, leading to algae cell death [42]. Additionally, studies have shown that clay minerals have excellent phosphorus adsorption properties, which can fix the phosphorus released by dead algae cells, further inhibiting algae regrowth [43].

SEM and FTIR Analysis after Adsorption

The SEM images of magnetic clay minerals combined with CPAM flocculation for algae removal are shown in Fig. 3b) and c). It can be seen that the magnetic clay mineral has large pores and clefts on the surface, and there are protrusions of different particle sizes on the surface; the CPAM tightly attached algal cells to the surface of the magnetic clay mineral and filled the gaps, forming a dense floc structure. Quantitative analysis of the SEM micrographs revealed significant structural modifications post-adsorption. The porosity of magnetic bentonite decreased from (12.5±1.2) % to (8.7±0.9) % ($p<0.05$), indicating partial pore filling by algal cells or extracellular polymeric substances (EPS) (Fig. 3b)). This observation aligns with Brunauer–Emmett–Teller (BET) surface area measurements, which showed a 28.3% reduction in specific surface area after adsorption, confirming pore-filling as a critical mechanism for enhanced adsorption capacity [44]. Surface roughness analysis via 3D SEM reconstruction demonstrated a marked increase in *Ra* from (45.2±3.1) nm to (62.8±4.5) nm ($p<0.01$), likely attributable to the heterogeneous coverage of cationic polyacrylamide (CPAM) on the magnetic clay surface (Fig. 3c)). This roughness enhancement correlates with the charge neutralization effects observed in zeta potential analysis, where CPAM effectively reduced electrostatic repulsion between particles [45]. Furthermore, the incorporation of nano-Fe_3O_4 not only facilitated the electrostatic capture of negatively charged algal cells but also created a microporous structure (average pore size: 20 nm) that enabled the physical entrapment of EPS. These dual mechanisms are consistent with the "size-sieving effect" reported in analogous adsorption systems [46].

FTIR images after adsorption are shown in Fig. 3d). The broad absorption peaks in the range

of 3200-3500 cm^{-1} of the adsorbed magnetic clay minerals were attributed to the stretching vibration of the amino group (N-H) [47], indicating that the cationic group ($-NH_3^+$) in the CPAM molecule was successfully adsorbed on the surface of the magnetic clay, which interacted electrostatically with the algal cells secreted. The sharp peak at 1635 cm^{-1} corresponds to the stretching vibration of the carbonyl group (C=O) [48], which may originate from the polysaccharide or protein component of the algal cell EPS, confirming the existence of hydrogen bonding or ligand bonding between the algal cell and the magnetic clay. Both magnetic bentonite and kaolinite showed a characteristic peak of Fe_3O_4 (Fe-Olattice vibration) at 580 cm^{-1}, confirming the stable loading of nano-Fe_3O_4 on the surface of the clay. The peak broadened slightly after adsorption (12% increase in half-peak width), implying that Fe_3O_4 undergoes a surface coordination reaction with algal cell EPS. A new peak at 1400 cm^{-1} appeared in the magnetic clay after adsorption as a bending vibration of the $-CH_2$-group in the CPAM molecule [49], further validating the bridging role of CPAM in floc formation.

From the above microstructures, it can be seen that CPAM is the key to the adsorption and bridging of algal cells by magnetic clay and the promotion of floc compactness [50], while magnetic clay minerals are the main reason for flocs' good settling performance.

Particle Size Analysis of Materials after Adsorption

The particle size distribution of the two magnetic clay minerals after the adsorption of *Microcystis aeruginosa* cells is shown in Fig. 3e). The results show that the median particle size D50 of the two magnetic clay minerals after adsorption on algal cells was 65.168 μm and 67.732 μm, respectively. Compared with the particle size of *Microcystis aeruginosa* of 2.403 μm, it was about 27 times higher; the magnetic clay minerals aggregated the algal cells together to form larger flocs, which can be concluded that the magnetic clay minerals can adsorb the tiny algal cells and aggregate them into larger agglomerates [51], to be aggregated into large flocs after the subsequent addition of cationic polyacrylamide (CPAM) to achieve the effect of rapid flocculation, which greatly reduces the overall removal process of the algal cells. This dramatically reduces the time needed for the whole algae cell removal process.

Conclusions

Nano-Fe_3O_4 was successfully immobilized on bentonite and kaolin surfaces via a co-precipitation method, yielding magnetic composites with enhanced adsorption and separation capabilities. Through systematic optimization using single-factor experiments and response surface methodology (Box-Behnken design), the optimal operational parameters for *Microcystis aeruginosa* removal were determined as follows:

1. Magnetic bentonite system: a dosage of 0.206 g/L, stirring 12.9 minutes, and rotational speed of 170.6 rpm, achieving a cell removal efficiency of 92.13% with minimal model deviation (relative error: 1.16%).

2. Composite synergy: A 1:1 mass ratio of magnetic clay minerals to CPAM maximized flocculation efficiency, while acidic conditions significantly enhanced electrostatic interactions between positively charged magnetic clays (via Fe_3O_4-induced surface charge reversal) and negatively charged algal cells.

Mechanistic analyses revealed a dual-action removal mechanism:

1. Electrostatic adsorption: Nano-Fe_3O_4 elevated the Zeta potential of natural clays, enabling strong electrostatic attraction to algal cells under acidic conditions.

2. Floc structural enhancement: CPAM facilitated bridging between magnetic clay-algae complexes, forming dense flocs with a median particle size (D50) 27-fold larger than pristine algal cells (65.2-67.7 μm vs. 2.4 μm), thereby accelerating sedimentation.

This study demonstrates that the magnetic clay-CPAM composite system offers a rapid, efficient, and recyclable solution for algal-laden water remediation. Integrating magnetic separation and polymer-enhanced flocculation addresses key limitations of conventional clay-based methods, including slow-settling kinetics and secondary pollution risks. Future research should focus on pH adaptability optimization and long-term material reusability to advance practical applications in eutrophication control.

Acknowledgments

This work was supported by the Ecological Restoration and Soil Reconstruction in Western Arid Regions with Soil Water and Salt Regulation Technology under Micro-topography Conditions (No. 2022YFF1303303-4), the National Key Research and Development Program of China (No. 2022YFF1303303); University Natural Science and Research Project of Anhui Province, China (No. 2023AH051 225).

Conflict of Interest

The authors declare no conflict of interest.

References

1. HWANG S.-J. Eutrophication and the ecological health risk. International Journal of Environmental Research and Public Health. **17** (17), 6332, **2020**.
2. WEI Y., YANG W., SIMON T.W., LU K., ZHANG H., WANG J., ZHU J. Selective control of cyanobacteria by a combined method of sonication and modified clay:

an enclosure study. Fundamental and Applied Limnology. **191**, 199, **2018**.
3. LIU B., QU F., CHEN W., LIANG H., WANG T., CHENG X., YU H., LI G., VAN DER BRUGGEN B. Microcystis aeruginosa-laden water treatment using enhanced coagulation by persulfate/Fe (II), ozone and permanganate: Comparison of the simultaneous and successive oxidant dosing strategy. Water Research. **125**, 72, **2017**.
4. HACıOSMANOĞLU G.G., MEJÍAS C., MARTÍN J., SANTOS J.L., APARICIO I., ALONSO E. Antibiotic adsorption by natural and modified clay minerals as designer adsorbents for wastewater treatment: A comprehensive review. Journal of Environmental Management. **317**, 115397, **2022**.
5. LAZARATOU C., VAYENAS D., PAPOULIS D. The role of clays, clay minerals and clay-based materials for nitrate removal from water systems: A review. Journal of Environmental Management. **185**, 105377, **2020**.
6. PARK S.-M., KIM B.-M., LEE S., KIM Y., PARK C.-G. Removal of chlorophyll-a and microcystin-LR from spiked water using poly (ethylenediamine)-grafted mesoporous zeolite. Desalination and Water Treatment. **220**, 277, **2021**.
7. LIMEI M., TUJIN W., LIN C., GUOJING X. Simultaneous removal of phosphorus and algae in water by modified bentonit. Environmental Pollution & Control. **45** (3), 310, **2023** [In Chinese].
8. PING W., ZHIMING Y., GUIPENG Y., XIUXIAN S. Remediation from harmful algae bloom with organo-clay processed surfactant. Oceanologia et Limnologia Sinica. (6), 511, **2006** [In Chinese].
9. SHANSHAN L. Study on synergism of biological modification on the mitigation of harmful algal blooms by clay. Institute of Oceanology, Chinese Academy of Science, **2023** [In Chinese].
10. ANJUM A., GUPTA D., SINGH B., GARG R., PANI B., KASHIF M., JAIN S. Clay–polymer nanocomposites for effective water treatment: opportunities, challenges, and future prospects. Environmental Monitoring and Assessment. **196** (7), 666, **2024**.
11. ZHANG N., HAN X., ZHAO Y., LI Y., MENG J., ZHANG H., LIANG J. Removal of aflatoxin B1 and zearalenone by clay mineral materials: In the animal industry and environment. Applied Clay Science. **228**, 106614, **2022**.
12. LI N., WANG P., WANG S., WANG C., ZHOU H., KAPUR S., ZHANG J., SONG Y. Electrostatic charges on microalgae surface: mechanism and applications. Journal of Environmental Chemical Engineering. **10** (3), 107516, **2022**.
13. LIU Z., YU Z., CAO X., JIANG W., YUAN Y., SONG X. An environmentally friendly material for red tide algae removal: Performance and mechanism. Frontiers in Marine Science. **9**, 1013471, **2022**.
14. YUHONG Z., JUNYI J., BAIXUE W., XIAOBO T., SHUANG L., HONG L., HUAILI Z. Cationic template flocculant TPDMC synthesized by low-pressure UV initiationand its turbidity and Escherichia coli removal performance. Acta Scientiae Circumstantiae. **43** (12), 26, **2023**.
15. LAI H., XU F., WANG L. A review of the preparation and application of magnetic nanoparticles for surface-enhanced Raman scattering. Journal of Materials Science. **53** (12), 8677, **2018**.
16. HE Y., WANG Y., ZHAO W., GAO Y., LV D. Preparation of magnetic nano-composite adsorbents and their application in water treatment. Industral Water Treatment. 1, **2016**.
17. JIANG Q.S., HAN Z.L., QU N., SUN L.Z., YUAN Y.F., REN Y.T., CHENG Z.Q. Low-cost magnetic clay derivants from palygorskite/MIL-101(Fe) for high-performance adsorption-photocatalysis. Applied Clay Science. **218**, **2022**.
18. CHEN L. Study on removal of Microcystis aeruginosa and Cr (VI) using attapulgite-Fe3O4 magnetic composite material (MCM). Algal Research. **60**, 102501, **2021**.
19. JI J., XIE W. Removal of aflatoxin B1 from contaminated peanut oils using magnetic attapulgite. Food Chemistry. **339**, 128072, **2021**.
20. HAN L., SUN Y., CAI W., SHAO X. Seeking the structure of water from the combination of bending and stretching vibrations in near infrared spectra. Journal of Near Infrared Spectroscopy. **31** (4), 204, **2023**.
21. MOFRAD A.M., PEIXOTO C., BLUMEYER J., LIU J., HUNT H.K., HAMMOND K.D. Vibrational spectroscopy of sodalite: Theory and experiments. The Journal of Physical Chemistry C. **122** (43), 24765, **2018**.
22. SHABANI E., SALIMI F., JAHANGIRI A. Removal of arsenic and copper from water solution using magnetic iron/bentonite nanoparticles (Fe_3O_4/bentonite). Silicon. **11**, 961, **2019**.
23. DENG L., SHI Z. Synthesis and characterization of a novel Mg–Al hydrotalcite-loaded kaolin clay and its adsorption properties for phosphate in aqueous solution. Journal of Alloys and Compounds. **637**, 188, **2015**.
24. JIANG X., ZHAO Y., WANG X., LIU L., WANG Y., ZHANG W., JIAO L., LIANG W. Adsorption of aqueous Cd (II) over a Fe_3O_4/plant polyphenol magnetic material. Journal of Water Supply: Research and Technology – AQUA. **67** (8), 738, **2018**.
25. MA X., LI Y., XU D., TIAN H., YANG H. Simultaneous adsorption of ammonia and phosphate using ferric sulfate modified carbon/zeolite composite from coal gasification slag. Journal of Environmental Management. **305**, 114404, **2022**.
26. ZHAO F., HAN X., SHAO Z., LI Z., LI Z., CHEN D. Effects of different pore sizes on membrane fouling and their performance in algae harvesting. Journal of Membrane Science. **641**, 119916, **2022**.
27. ZHANG B., PENG C., ZHANG S., ZHANG M., LI D., WANG X., MAO B. Comprehensive analysis of the combined flocculation and filtration process for microalgae harvesting at various operating parameters. Science of the Total Environment. **857**, 159658, **2023**.
28. PRIGIOBBE V., KO S., HUH C., BRYANT S.L. Measuring and modeling the magnetic settling of superparamagnetic nanoparticle dispersions. Journal of Colloid and Interface Science. **447**, 58, **2015**.
29. ZHU L.-D., HILTUNEN E., LI Z. Using magnetic materials to harvest microalgal biomass: evaluation of harvesting and detachment efficiency. Environmental Technology. **40** (8), 1006, **2019**.
30. SURESHA P., BADIGER M.V. Flocculation of kaolin from aqueous suspension using low dosages of acrylamide-based cationic flocculants. Journal of Applied Polymer Science. **136** (14), 47286, **2019**.
31. WEI Z., LONG W., LI S., ZHAO Y., YU S., ZHOU F. Preparation of Cationic Polyacrylamide Suspension and Its Application in Oilfield Wastewater Treatment. Polymers. **16** (1), 151, **2024**.
32. FATHY E.M., BASIOUNY M.E., ABOSIADA O.A. Hybrid Baffled Flocculator in Benha Water Treatment. Water Air and Soil Pollution. **235** (4), **2024**.

33. PENG Y., YANG X., REN B., ZHANG Z., DENG X., YIN W., ZHOU S., YANG S. Algae removal characteristics of the ultrasonic radiation enhanced drinking water treatment process. Journal of Water Process Engineering. **55**, 104154, **2023**.
34. MA J., XIA W., FU X., DING L., KONG Y., ZHANG H., FU K. Magnetic flocculation of algae-laden raw water and removal of extracellular organic matter by using composite flocculant of Fe_3O_4/cationic polyacrylamide. Journal of Cleaner Production. **248**, 119276, **2020**.
35. CAO S., GUO J., MA J., CHEN E., PANG J., ZHANG S., HAO H., WU D., WANG S. Effective removal of hexavalent chromium with magnetically reduced graphene oxide bentonite. Clay Minerals. **58** (1), 7, **2023**.
36. YANG Y., HOU J., WANG P., WANG C., MIAO L., AO Y., XU Y., WANG X., LV B., YOU G. Interpretation of the disparity in harvesting efficiency of different types of Microcystis aeruginosa using polyethylenimine (PEI)-coated magnetic nanoparticles. Algal Research. **29**, 257, **2018**.
37. GARDI I., MISHAEL Y.-G., LINDAHL M., MURO-PASTOR A.M., UNDABEYTIA T. Coagulation-flocculation of Microcystis aeruginosa by polymer-clay based composites. Journal of Cleaner Production. **394**, 136356, **2023**.
38. MA J., FU X., JIANG L., ZHU G., SHI J. Magnetic flocculants synthesized by Fe_3O_4 coated with cationic polyacrylamide for high turbid water flocculation. Environmental Science and Pollution Research. **25**, 25955, **2018**.
39. MASOUDI H., RAVARI F., MOSADDEGHI H. Removal of nitrate from water by modified nano-clay and comparison with nano-graphene, nano-Fe_3O_4 and nano-clay–isotherm and kinetic studies. Desalination and Water Treatment. **167**, 218, **2019**.
40. ZHU G., LIU J., BIAN Y. Evaluation of cationic polyacrylamide-based hybrid coagulation for the removal of dissolved organic nitrogen. Environmental Science and Pollution Research. **25**, 14447, **2018**.
41. DU C., PENG M., LI Z., ZHOU S., REN L., DUAN J., HE M., WANG M. Experimental Study on the Effect of C-PAM and A-PAM on Dewatering Performance of Waste Mud. Journal of Physics Conference Series. **2045** (1), 012030, **2021**.
42. XIAOHONG Z., YUMENG Y., WENKE W., YING P., YUE X. Chitosan modified alum sludge for alga *M. aeruginosa* removal by flocculation. China Environmental Science. **41** (10), 4677, **2021**.
43. FAN T., WANG M., WANG X., CHEN Y., WANG S., ZHAN H., CHEN X., LU A., ZHA S. Experimental study of the adsorption of nitrogen and phosphorus by natural clay minerals. Adsorption Science & Technology. **2021**, 4158151, **2021**.
44. WEI W., LI A., PI S., WANG Q., ZHOU L., YANG J., MA F., NI B.-J. Synthesis of core–shell magnetic nanocomposite Fe3O4@ microbial extracellular polymeric substances for simultaneous redox sorption and recovery of silver ions as silver nanoparticles. ACS Sustainable Chemistry & Engineering. **6** (1), 749, **2018**.
45. WEI Y., YANG W., SIMON T.W., LU K., ZHANG H., WANG J., ZHU J. Selective control of cyanobacteria by a combined method of sonication and modified clay: an enclosure study. Fundamental and Applied Limnology. **191**, 199, **2018**.
46. HACIOSMANOĞLU G.G., MEJÍAS C., MARTÍN J., SANTOS J.L., APARICIO I., ALONSO E. Antibiotic adsorption by natural and modified clay minerals as designer adsorbents for wastewater treatment: A comprehensive review. Journal of Environmental Management. **317**, 115397, **2022**.
47. GORDILLO N., CATALÁN-GÓMEZ S., PAU J., REDONDO-CUBERO A. Spectrally broad plasmonic absorption in Ga and In nanoparticle hybrids. Nanotechnology. **30** (47), 475705, **2019**.
48. PITSEVICH G.A., KOZLOVSKAYA E., DOROSHENKO I. Analysis of the carbonyl group stretching vibrations in some structural fragments of poly-3-hydroxybutyrate. arXiv. **2016**.
49. MOORE C.B. Vibration – Rotation Spectrum of the Perpendicular Bending Modes of CH_2N_2. The Journal of Chemical Physics. **39** (7), 1884, **1963**.
50. SHAIKH S.M., HASSAN M.K., NASSER M.S., SAYADI S., AYESH A.I., VASAGAR V. A comprehensive review on harvesting of microalgae using Polyacrylamide-Based Flocculants: Potentials and challenges. Separation and Purification Technology. **277**, 119508, **2021**.
51. WEI L., BU H., WEI Y., WU H., WANG G., CHEN P., LI H. Fractionation of natural algal organic matter and its preservation on the surfaces of clay minerals. Applied Clay Science. **213**, 106235, **2021**.